JACS
JOURNAL OF THE AMERICAN CHEMICAL SOCIETY

Article

pubs.acs.org/JACS

Electrostatic and Allosteric Cooperativity in Ion-Pair Binding: A Quantitative and Coupled Experiment–Theory Study with Aryl–Triazole–Ether Macrocycles

Bo Qiao, Arkajyoti Sengupta, Yun Liu, Kevin P. McDonald, Maren Pink, Joseph R. Anderson, Krishnan Raghavachari, and Amar H. Flood*

Department of Chemistry, Indiana University, 800 East Kirkwood Avenue, Bloomington, Indiana 47405, United States

Supporting Information

ABSTRACT: Cooperative binding of ion pairs to receptors is crucial for the manipulation of salts, but a comprehensive understanding of cooperativity has been elusive. To this end, we combine experiment and theory to quantify ion-pair binding and to separate allostery from electrostatics to understand their relative contributions. We designed aryl–triazole–ether macrocycles (**MC**) to be semiflexible, which allows ion pairs (NaX; X = anion) to make contact, and to be monocyclic to simplify analyses. A multiequilibrium model allows us to quantify, for the first time, the experimental cooperativity, α, for the equilibrium **MC**·Na^+ + **MC**·X^- ⇌ **MC**·NaX + **MC**, which is associated with contact ion-pair binding of NaI (α = 1300, $\Delta G_\alpha = -18$ kJ mol^{-1}) and $NaClO_4$ (α = 400, $\Delta G_\alpha = -15$ kJ mol^{-1}) in 4:1 dichloromethane–acetonitrile. We used accurate energies from density functional theory to deconvolute how the electrostatic effects and the allosteric changes in receptor geometry individually contribute to cooperativity. Computations, using a continuum solvation model (dichloromethane), show that allostery contributes ~30% to overall positive cooperativity. The calculated trend of electrostatic cooperativity using pairs of spherical ions (NaCl > NaBr > NaI) correlates to experimental observations (NaI > $NaClO_4$). We show that intrinsic ionic size, which dictates charge separation distance in contact ion pairs, controls electrostatic cooperativity. This finding supports the design principle that semiflexible receptors can facilitate optimal electrostatic cooperativity. While Coulomb's law predicts the size-dependent trend, it overestimates electrostatic cooperativity; we suggest that binding of the individual anion and cation to their respective binding sites dilutes their effective charge. This comprehensive understanding is critical for rational designs of ion-pair receptors for the manipulation of salts.

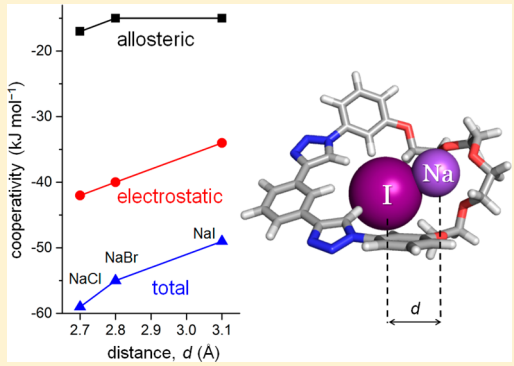

INTRODUCTION

Cooperativity is a powerful strategy for forming high-fidelity species[1] during molecule-mediated recognition of ion pairs[2] and for effecting allosteric control over binding events.[3] Such ion-pair recognition has many applications, including ion extraction,[4] membrane transport,[5] and catalysis.[6] Despite these many roles, ion complexation has primarily focused on the binding of cations[7] and anions[8] individually. The associated counterions have often gone unobserved[9] or overlooked, yet it has become increasingly apparent that these counterions play critical roles[9−11] in complexation events. When ion-pair binding is examined specifically, such as in cascade complexes[12] and ion-pair receptors,[13] synergistic effects exist and offer a means to modulate strength, selectivity, and population fidelity.[14] A quantitative account of the factors that dictate these synergies will allow for an understanding of the behaviors of ion pairs in various applications[4−6] and for the design of receptors with targeted selectivities. However, quantitative studies in previous literature that outline the geometric and electrostatic contributions to the cooperativity are rare. Obtaining a comprehensive picture of ion-pair binding is challenging to achieve due to the need to identify and then evaluate multiple equilibria[4b] that represent all the important supramolecular processes. We do this here using a coupled experiment–theory approach[11c,15−18] and distinguish, for the first time, allostery from electrostatics to help reveal the fundamental features controlling and benefitting electrostatic cooperativity when using semiflexible ion-pair receptors (Figure 1).

There are two accepted mechanisms[13] by which cooperativity can emerge in ion-pair binding: conformational allostery and electrostatic. With *positive* conformational allostery, binding the cation helps organize the receptor for the anion, thus the geometrical deformation penalty is lower for binding the ion pair than for either cation and anion separately.[10,19] Electrostatic cooperativity is expected to come from the attraction, E_{Coul}, between the anion and cation inside the receptor[20] and to be governed by Coulomb's law,[21]

$$E_{Coul} = q_1 q_2 / 4\pi\varepsilon_0 \varepsilon d \quad (1)$$

Received: June 10, 2015
Published: July 24, 2015

DOI: 10.1021/jacs.5b05839
J. Am. Chem. Soc. 2015, 137, 9746–9757

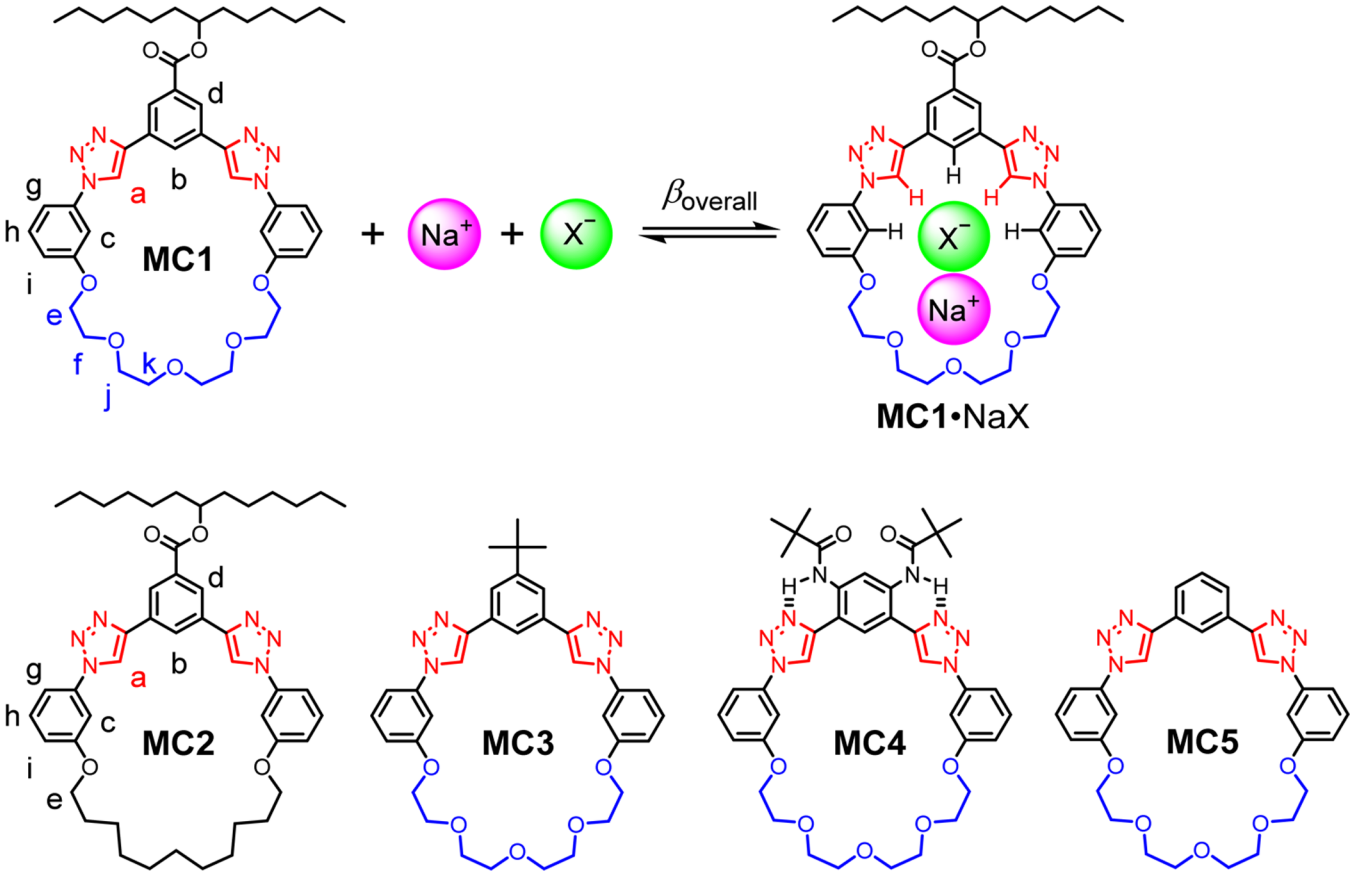

Figure 1. Chemical structures of the macrocycles and principal equilibrium studied in this work. Macrocycle **MC1** for ion-pair binding bears extrinsically polarized triazoles (red) for CH hydrogen-bonding to anions and the ethylene glycol ether (blue) for cations. **MC2** serves as an anion-only control receptor, **MC3** and **MC4** for crystal structure determinations, and **MC5** for computational studies.

where q_1 and q_2 are the charges on the cation and anion, d is the cation−anion distance, ε_0 is the permittivity of vacuum, and ε is the dielectric constant of the medium.

Many but not all[15b,19,22] of the literature examples of ion-pair binding used phenomenological turn-on factors to demonstrate positive cooperativity. Therein, an anion's *apparent* affinity for the receptor increases when an appropriate cation is premixed with the receptor. Using turn-on factors, Reinhoudt demonstrated conformational allostery in a calix[4]arene receptor,[19a] Smith showed the benefits of reducing cavity size for binding NaCl with bicyclic amide−crown-ether receptors,[20a,23] and Beer explored allosteric selectivity as dictated by the stoichiometry of cation binding of a calix[4]arene crown-ether receptor.[24] Other studies have built on these lessons.[13,25] However, and as Roelens[26] noted, this turn-on method of evaluation is phenomenological and, therefore, does not provide the thermodynamic data needed for accurately determining the origin and strength of cooperativity in ion-pair binding.

Quantification of cooperativity is all-important for the understanding and rational design of ion-pair receptors with desired affinity and selectivity. Recent works have started to reveal more detail. Using experiment, Ballester treated ion pairs as entire guests in a model set of equilibria to analyze the cooperativity of multiple ion-pair binding to a bis(calix[4]-pyrrole) receptor.[22b] Sessler and Moyer established multi-equilibria models to characterize biphasic, liquid−liquid extractions of radioactive ions by calix[4]pyrrole receptors.[4a] Using theory, Sessler and Hay[20b] optimized geometries of an ion-pair complex to a calix[4]pyrrole−crown-ether receptor to analyze various binding modes, and Dutasta[27] calculated the cation−anion distances of ion pairs in a hemicryptophane receptor to explain the observed selectivity. These recent works provided more quantitative detail than the turn-on factors and deepened our understanding of ion-pair binding but did not directly focus on the origin of the cooperativity within the 1:1:1 complexes formed between cation, anion, and receptor.

There are several challenges facing a full quantitative investigation of cooperativity in ion-pair binding. First, ion-pair binding involves multiple equilibria that demand sophisticated binding models and rely upon several affinity measurements of contributing equilibria. Some of those experiments can be limited by the solubility of the salts or the binding strength of the receptors.[4b] Second, both conformational and electrostatic factors contribute to the net cooperativity displayed during ion-pair binding. It is almost impossible to deconvolute these two factors from each other using experiment alone. Yet, all these challenges need to be overcome in order to provide a comprehensive picture of cooperativity in ion-pair binding.

We address these challenges by pairing experiment with theory to quantify cooperativity of binding ion pairs ($NaClO_4$, NaI, NaBr, and NaCl) inside a ditopic aryl−triazole−ether macrocycle (**MC1**, Figure 1). Instead of using turn-on factors, we employed an accurate binding model[4b,26] that faithfully represents all the important equilibria present in solution. These include anion binding, K_{anion}, cation binding, K_{cation}, and

DOI: 10.1021/jacs.5b05839
J. Am. Chem. Soc. 2015, 137, 9746−9757

Scheme 1. Modular Synthesis of Macrocycles MC1, MC2, MC3, and MC4 (TBTA = tris[(1-benzyl-1*H*-1,2,3-triazol-4-yl)methyl]amine)

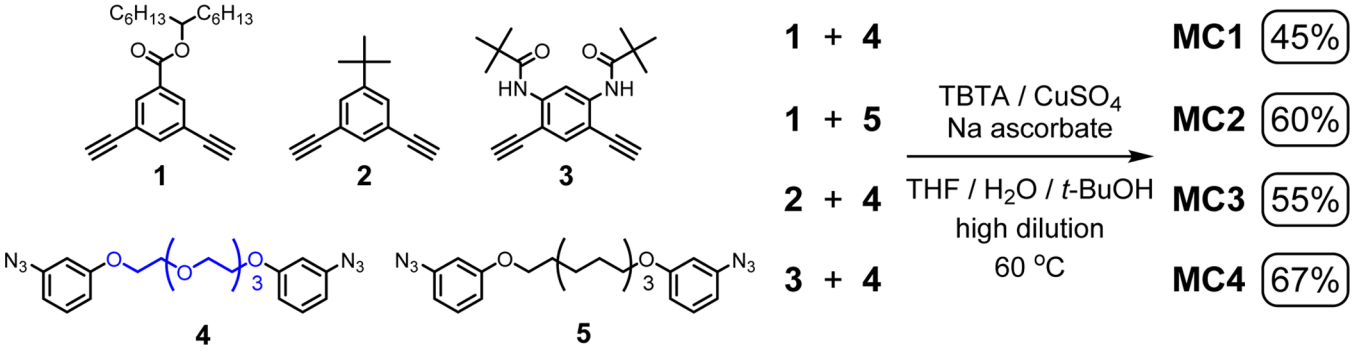

the ternary ion-pair binding, $\beta_{overall}$ (Figure 1), from which we determine the cooperativity factor, α:

$$\alpha = \beta_{overall}/K_{anion}K_{cation} \quad (2)$$

Cooperativity factors that are greater than 1 indicate additional stabilization is present within the ternary ion-pair complex, i.e., positive cooperativity. We determined the cooperativity factors in solution-phase experimental studies involving $NaClO_4$ and NaI binding. In a complementary manner, we established a set of quantum chemical calculations to investigate cooperativity across an overlapping range of ion-pairs (NaCl, NaBr, and NaI). These are examined both in the gas phase and with the inclusion of a continuum solvation model. A distinct benefit of the theoretical approach is that the deformation penalty, D_{ion}, associated with all the binding events can be explicitly calculated allowing us to determine conformational cooperativity, also known as allostery, in ion-pair binding for the first time. Thus, we have also determined the pure electrostatic contribution to the overall cooperativity for the first time. It was found that when our semiflexible ion-pair receptor allows the ion pairs to have close contact, they display their "intrinsic" electrostatic cooperativity in a manner that depends on the size of the ions: smaller ions will naturally have higher cooperativity. While Coulombic interactions are expected to be proportional to $1/d$, to the best of our knowledge, this is the first quantitative and comprehensive examination of this idea in ion-pair binding. Overall, these insights help establish a quantitative basis for both the design of ion-pair receptors and the understanding of how ion pairs engage with functional molecules.[4−6,28]

METHODS

^{1}H NMR Titrations. Titrations were conducted with **MC1** to determine equilibrium constants. All titrations were conducted by adding increasing amounts of the corresponding salt into solutions of **MC1** or **MC2** (2 mM, 4:1 *v*/*v* CD_2Cl_2:CD_3CN). Titration data were monitored by ^{1}H NMR spectroscopy (500 MHz) at room temperature (298 K). In a typical experiment, 500 μL of a 2 mM macrocycle solution was prepared in screw-cap NMR tubes equipped with PTFE/silicone septa. Aliquots from a 40 mM salt solution in a screw-cap vial equipped with PTFE/silicone septa were added using 10 and 100 μL gastight microsyringes.

DFT Calculations. All computations have been carried out using the Gaussian suite of programs.[29] The starting geometries were obtained from the crystal structures and optimized with the widely used M06-2X functional[30] both in the gas phase and with CH_2Cl_2 solvation based on the IEFPCM model (integral equation formalism polarizable continuum model).[31] Optimized geometries, vibrational frequencies, zero-point energy corrections, and thermal corrections have been evaluated using the 6-31+G(d,p) basis set on the first- and second-row elements, and the LANL2DZdp basis set (which bears an extra set of diffuse and polarization functions) on bromine and iodine.[32] All geometries were confirmed to be minima with no imaginary frequencies. Single-point energy calculations were carried out subsequently using the significantly larger 6-311++G(3df,2p) basis sets to obtain the binding energies with greater accuracy. Single-point implicit solvent computations were performed on the optimized geometries at the M06-2X/6-311++G(3df,2p) level of theory. Since the larger basis set was not previously available for iodine, an appropriate basis set was constructed by addition of a set of diffuse s and p functions, two d functions, and one f function to the 6-311G(d) basis set for iodine.

RESULTS AND DISCUSSION

Design and Synthesis of Aryl−Triazole−Ether Receptors for Ion Pairs. A heteroditopic macrocycle was designed for binding contact ion pairs. The macrocycle combines a rigid aryl−triazole crescent[9a,18d,33] for binding anions together with a glycolic linker for stabilizing cations. In contrast to the more common use of *poly*cyclic receptors[13] designed to achieve unique affinities and/or selectivities, the simplicity of this *mono*cyclic structure will greatly aid in the analysis of cooperativity. We also expect the modest cavity size and the flexibility of the glycol chain to ensure that, once the ions are bound inside the receptor, they will make direct contact with each other.

The various macrocycles (Figure 1) all share a central core and are customized for specific purposes. Macrocycle **MC1** bears long solubilizing side chains for solution-phase binding studies. While **MC1** is designed to be a receptor for ion pairs, **MC2** is a control molecule in which the cation-binding glycols have been replaced with an isosteric non-interacting alkyl chain. Therefore, it represents an anion-only receptor. Macrocycles **MC3** and **MC4** with bulky *tert*-butyl side groups were designed for growing single crystals for X-ray diffraction. With **MC5**, all the side chains were removed for the purpose of simplifying the computational studies.

All the macrocycles investigated experimentally were prepared (Scheme 1) from the copper-catalyzed azide−alkyne cycloadditions[34] between bis-alkynyl phenylenes and bis-azido chains in high dilution conditions. Phenylenes **1**, **2**, and **3** were prepared according to reported procedures,[11c,33c] and building blocks **4** and **5** were prepared in three steps from 3-iodophenol.[35]

Qualitative Analysis of Ion-Pair Binding. The heteroditopic character of the receptor's design was made evident from the electrostatic potential (ESP) map[18b] of macrocycle **MC3** (Figure 2a) and its solid-state structure complexed with a

DOI: 10.1021/jacs.5b05839
J. Am. Chem. Soc. 2015, 137, 9746−9757

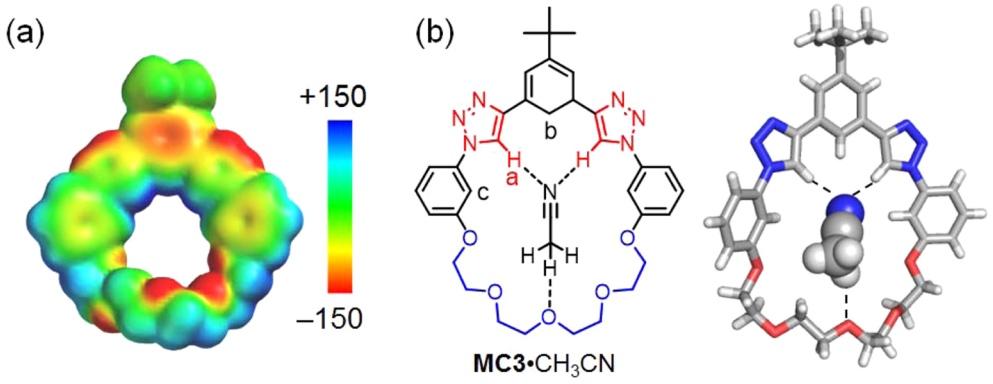

Figure 2. (a) Electrostatic potential map of **MC3** (HF/3-21G*). (b) Chemical and solid-state structure of **MC3**·CH_3CN with short-distance (<3.0 Å) hydrogen bonds marked.

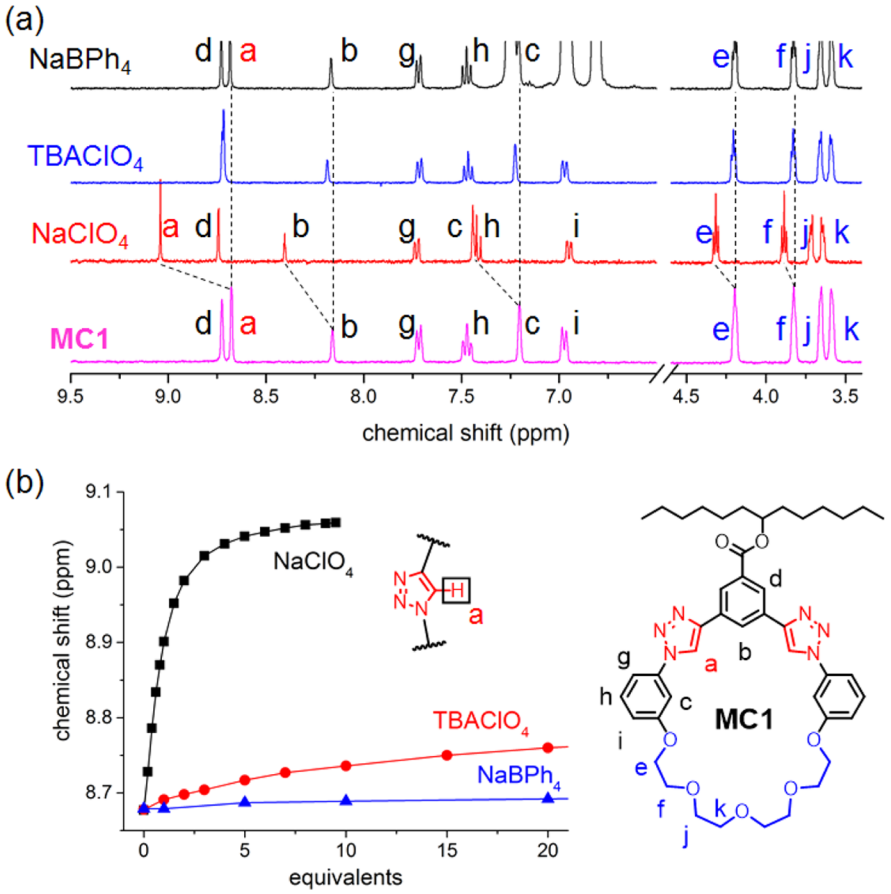

Figure 3. (a) ^1H NMR spectra of **MC1** (2 mM, 4:1 CD_2Cl_2:CD_3CN, 500 MHz, 298 K) with five equivalents of $NaBPh_4$ (black), $TBAClO_4$ (blue), and $NaClO_4$ (red) compared to the free receptor (magenta). (b) ^1H NMR chemical shifts of the triazole proton H_a in **MC1** with increasing equivalents of the various salts.

solvent molecule **MC3**·CH_3CN (Figure 2b). An ordered acetonitrile molecule forms short CH···N (2.6 Å) hydrogen bonds from the anion-binding triazoles (colored red) and CH···O (2.6 Å) hydrogen bonds to the cation-binding ether oxygens at the glycol end of the cavity. The parent macrocycle **MC1** has essentially the same ESP map as **MC3**. Based on spatial ^1H–^1H couplings between protons H_a, H_b, and H_c observed in the NOESY NMR spectra[18d,33] of **MC1** (Supporting Information), the geometry of macrocycle **MC1** is believed to be the same as the macrocycle in the **MC3**·CH_3CN crystal. Thus, **MC1** is preorganized with the triazole CH bond donors pointing into the central cavity.

To begin, cooperative ion-pair binding was found to be present when studying qualitatively the binding of $NaClO_4$ with macrocycle **MC1** (Figure 3). The peak shifts in the ^1H NMR spectra accompanying the addition of $NaClO_4$ were compared to shifts for addition of the constituent ions (Na^+ or ClO_4^-) when they were added "alone". The Na^+ was added as the tetraphenylborate (BPh_4^-) salt and ClO_4^- as the tetrabutylammonium (TBA^+) salt. These counterions are too large to associate with the receptor. A 4:1 mixture of CD_2Cl_2 and

DOI: 10.1021/jacs.5b05839
J. Am. Chem. Soc. 2015, 137, 9746–9757

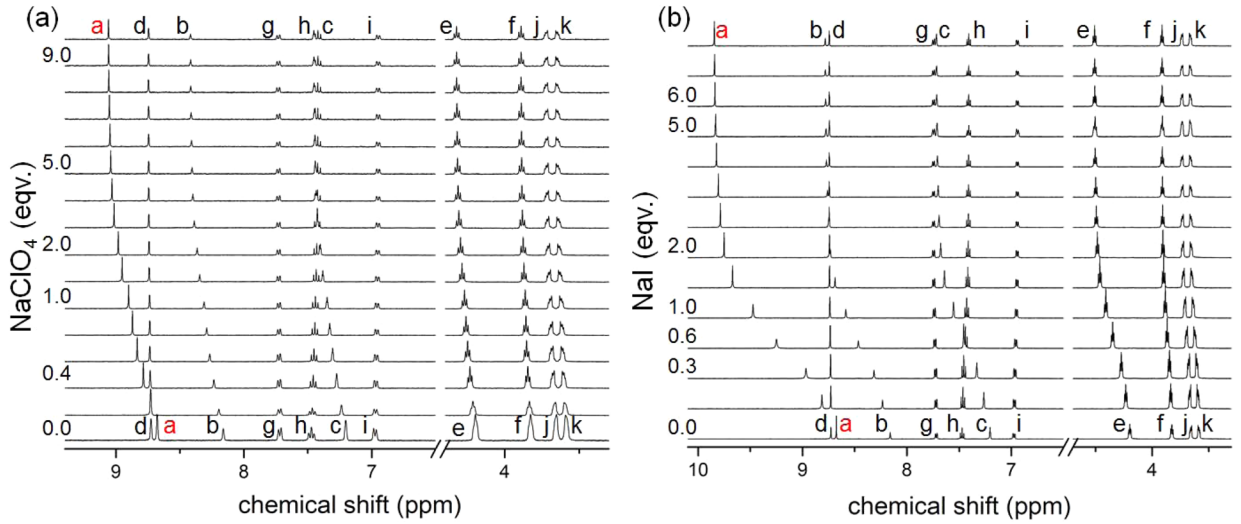

Figure 4. Stacked ^{1}H NMR spectra of **MC1** with increasing amounts of (a) $NaClO_4$ and (b) NaI. Conditions: [**MC1**] = 2 mM, 4:1 CD_2Cl_2:CD_3CN, 298 K, 500 MHz.

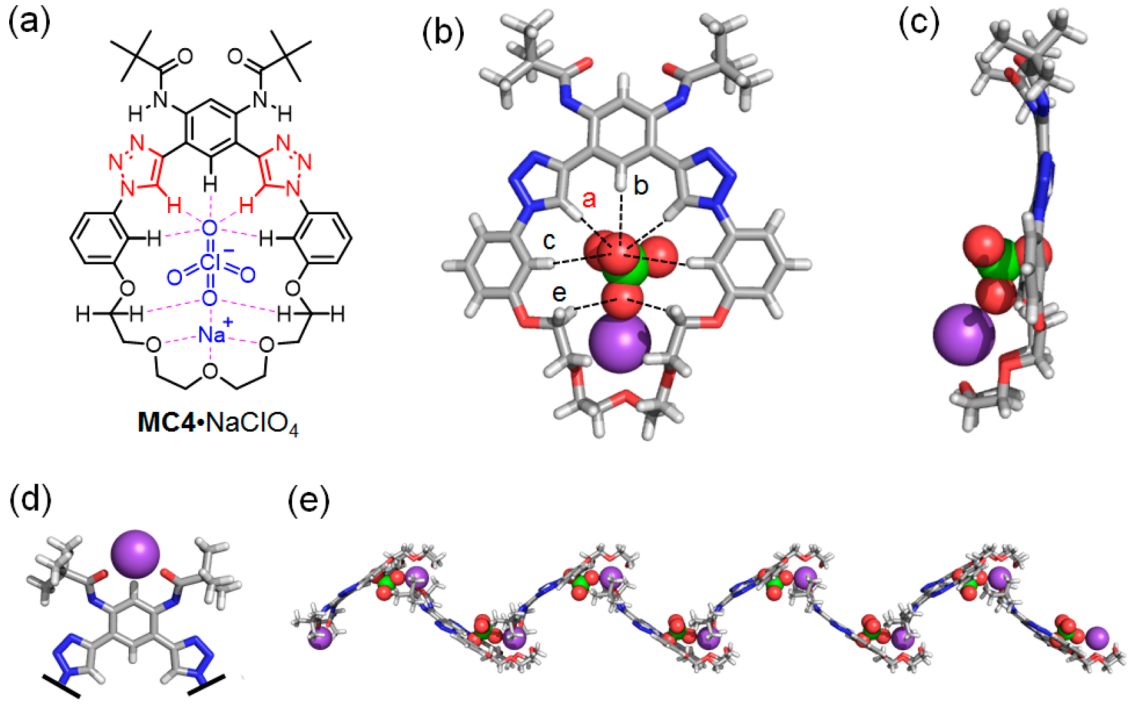

Figure 5. (a) Chemical structure of **MC4**·$NaClO_4$ highlighting short contacts (dashed pink lines). (b) Top and (c) side views of solid-state structure of **MC4**·$NaClO_4$. (d) Upper part of the structure highlighting the exterior Na^+ binding site of **MC4**. (e) A supramolecular polymer formed by **MC4**·$NaClO_4$ monomers in the solid state. Solvent molecules removed for clarity.

CD_3CN was used to provide good solubility to both the receptor and all titrated salts. Addition of 5 equiv of either the Na^+ cation ($NaBPh_4$) or the ClO_4^- anion ($TBAClO_4$) to macrocycle **MC1** did not show significant changes to the ^{1}H NMR spectra (2 mM, Figure 3a), indicative of weak individual binding. However, upon addition of the $NaClO_4$ ion pair (Figure 3a), many of the protons shift to new positions indicative of complex formation. The protons in the electropositive anion-binding cavity of **MC1** (H_a, H_b, and H_c) shift downfield consistent with CH···anion hydrogen-bonding. The ethylene glycol's signals also shift downfield with the presence of $NaClO_4$ (Figure 3a, H_f, H_j, H_k), which is consistent with prior NMR analyses of alkali cation binding to crowns.[36]

The strong binding of $NaClO_4$ to **MC1** and weak binding of ClO_4^- and Na^+ was further verified by adding increasing amounts of their respective salts to solutions of **MC1**. Addition of $NaClO_4$ (Figure 4a) induces H_a to shift until saturation is achieved just prior to 5 equiv, indicative of complete conversion from free **MC1** to the **MC1**·$NaClO_4$ complex. A comparison of $NaClO_4$ binding to those of the constituent ions, ClO_4^- and Na^+ (Figure 3b), shows that when the ions are alone they do not saturate the receptor. The same experiments were carried out to test binding of the iodide version, NaI, and the result was similar: strong NaI binding to **MC1** (Figure 4b) but weak binding of the I^- anion and Na^+ cation alone (Supporting Information). The saturation seen for the ion pairs relative to

DOI: 10.1021/jacs.5b05839
J. Am. Chem. Soc. 2015, 137, 9746−9757

the constituent ions (Figure 3b) is a qualitative indicator of cooperativity.

The X-ray structure of the ion-pair complex with macrocycle **MC4** (Figure 5) confirms the formation of a contact ion pair inside the cavity. The solid-state structure shows $NaClO_4$ perches in the receptor pocket and that neither anion nor cation has a perfect fit for the cavity. Only one oxygen atom in the perchlorate is in close contact with the five CH hydrogen bond donors within the electropositive end of the cavity (CH···O distances range from 2.4 to 3.2 Å). Furthermore, sodium does not appear to be an ideal guest for the cation pocket; only three of the possible five Na^+···O close contacts are formed with distances ranging from 2.3 to 3.0 Å. The nonideal fit of either ion into their half of the binding cavity is consistent with the poor binding seen for the ions alone (Figure 3).

The cation and anion sit close to each other inside this macrocycle. The Na···O distance of the bound $NaClO_4$ ion pair is 2.3 Å, and the Na···Cl distance is 3.6 Å. These distances can be compared to the few organic crystals identified in the Cambridge Structure Database in which $NaClO_4$ is also being stabilized by other non-covalent interactions. Most of these involve the Na^+ cation bound by a receptor with the ClO_4^- paired to the cation but residing outside the receptor. In these cases, the sodium−oxygen distance (Na···O−ClO_3^-) ranges from 2.3 to 3.0 Å.[37] The crystal structure of **MC4**·$NaClO_4$ showing $NaClO_4$ nestled in the receptor may be the first of its kind. Overall, these short cation−anion distances are indicative of strong electrostatic interactions.

The $NaClO_4$ complex also shows the formation of CH··· anion hydrogen bonds that involve the methylene CH groups from the glycol chain (H_e, Figure 5). Compared to the crystal structure of **MC3**·CH_3CN, the methylene CH groups appear to have redirected inside the cavity. Presumably, this interaction[11c,38] also offers additional stabilization to the ion-pair complex. ^{1}H NMR titration data of **MC1** with $NaClO_4$ showed (Figure 4a) a downfield shift in proton H_e that is consistent with such an interaction being present in solution.[39]

An unexpected feature present in the crystal structure involves chelation of the sodium cation by the two amide carbonyl groups of a *neighboring* **MC4** (Figure 5d) enabling the formation of a 1D supramolecular polymer (Figure 5e). The existence of this second *external* Na^+ binding site was verified in solution by ^{1}H NMR titration of $NaBPh_4$ and $NaClO_4$ with **MC4**, showing Na^+ cations occupying both sites (Supporting Information). We believe this binding site enhances the perched binding mode. For all these reasons, the quantitative solution-phase studies were conducted using **MC1**, which does not have this external site.

Macrocycle **MC4** was also found to bind NaI in the solid state (Figure 6) with almost exactly the same geometry as $NaClO_4$ (Figure 5). The close contact distance between Na^+ and I^- is 3.2 Å, which falls within the range of Na^+···I^- contact ion-pair distances (2.9−3.6 Å) seen in other NaI complexes with organic molecules.[40] Furthermore, the structural similarity allows any energetic differences between $NaClO_4$ and NaI to be rationalized from electrostatics.

With the two ions in direct contact, both complexes are expected to benefit from electrostatic attraction, however, the extent of such stabilization has never been rigorously tested. For $NaClO_4$ and NaI in our solution conditions[41] ($\varepsilon \approx 16.1$ for 4:1 CH_2Cl_2:CH_3CN) and using the distances obtained from the crystals, it is hypothesized from Coulomb's law that they should be cooperatively stabilized by ~25 kJ mol^{-1}. To test this idea, to quantify cooperativity, and to reveal its origins, we require models for interpreting the experimental and computational data.

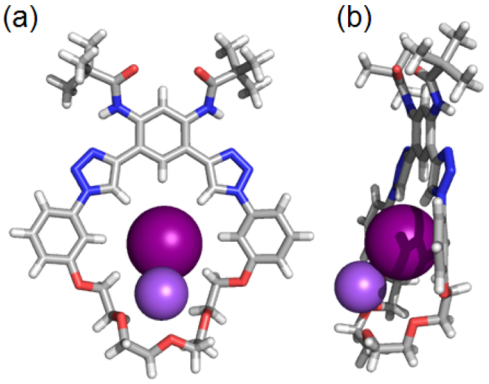

Figure 6. Solid-state structure of **MC4**·NaI in (a) front and (b) side views.

Model for Cooperative Ion-Pair Binding. An appropriate binding model (eqs 3−5) to analyze how ion pairs bind to receptors needs to include three independent equilibria: anion binding, K_{anion}, cation binding, K_{cation}, and the overall 1:1:1 ternary binding, $\beta_{overall}$:

$$\mathbf{MC} + X^- \rightleftharpoons \mathbf{MC}\cdot X^- \qquad K_{anion} \quad (3)$$

$$\mathbf{MC} + M^+ \rightleftharpoons \mathbf{MC}\cdot M^+ \qquad K_{cation} \quad (4)$$

$$\mathbf{MC} + M^+ + X^- \rightleftharpoons \mathbf{MC}\cdot MX \qquad \beta_{overall} \quad (5)$$

The cooperativity factor, α, is the overall binding constant divided by the product of ion binding (eq 2). The associated free energy, ΔG_α, is defined as the overall binding, $\Delta G_{overall}$, minus the anion and cation binding free energies, ΔG_{anion} and ΔG_{cation}:

$$\Delta G_\alpha = \Delta G_{overall} - \Delta G_{anion} - \Delta G_{cation} \quad (6)$$

The cooperativity parameters, α and ΔG_α, are the equilibrium constant and the free energy associated with the following reaction:

$$\mathbf{MC}\cdot X^- + \mathbf{MC}\cdot M^+ \rightleftharpoons \mathbf{MC}\cdot MX + \mathbf{MC} \qquad \alpha, \Delta G_\alpha \quad (7)$$

When ΔG_α is less than zero (Figure 7), products are favored by an additional stabilization that is only present when the ions are bound as a pair. On the basis of eq 6, if the three binding energies (anion, cation, and overall) can be determined individually, either by experiment or by theoretical calculations, then the cooperativity, ΔG_α, can be quantitatively obtained.

Model for Electrostatic and Allosteric Cooperativity. Cooperativity can be further deconvoluted into its components to start building a comprehensive understanding of its origin. It is generally assumed that there are cooperativity contributions arising from electrostatic stabilization, ΔG_{elec}, and from conformational allostery, ΔG_{allos}:

$$\Delta G_\alpha = \Delta G_{elec} + \Delta G_{allos} \quad (8)$$

We believe that the electrostatic cooperativity is straightforward to describe as the additional attraction energy between cation and anion when they are bound at the same time (Figure 8a). All ion-pair receptors that bring their cation and anion reasonably close to each other are expected to benefit from this type of stabilization.

DOI: 10.1021/jacs.5b05839
J. Am. Chem. Soc. 2015, 137, 9746−9757

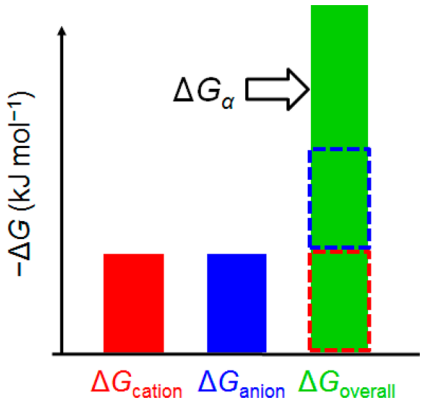

Figure 7. Representation of the additional free energy, ΔG_α, under conditions of positive cooperativity, that emerges when comparing the overall free energy of binding the ion pair to the sum of binding the cation and anion individually.

The conformational contribution to cooperativity is less obvious and has not, to the best of our knowledge, been rigorously investigated. We define conformational cooperativity, ΔG_{allos} (eq 9, Figure 8b), from the difference in deformation energy, D_i, within reaction 7. Any individual deformation energies, D_i, are always going to be penalties because perfect preorganization is an unattainable ideal. These energies are associated with reorganizing the receptor upon binding the guest (Figure 8b). Thus, the difference between the overall deformation penalty, $D_{overall}$ (for binding the ion pair), and the sum of cation and anion deformation penalties, $D_{cation} + D_{anion}$ (for binding cation and anion individually), defines ΔG_{allos}:

$$\Delta G_{allos} = D_{overall} - D_{cation} - D_{anion} \quad (9)$$

If the deformation penalty of binding the whole ion pair is less than the penalty of binding the anion and the cation individually, then it is more beneficial to bind the ions as a pair. This benefit corresponds to positive conformational allostery. Irrespective of whether the conformational cooperativity is positive or negative, it is almost universally present since it is extremely unlikely for $D_{overall}$ to equate to $D_{anion} + D_{cation}$.

With the models developed here for determining the cooperativity and deconvoluting it into its two components, we now present the data and its analysis.

Experimental Analysis of the Cooperativity. Experimentally, the extent of cooperativity, ΔG_α, can be determined after ΔG_{anion}, ΔG_{cation}, and $\Delta G_{overall}$ for equilibria 3−5 are all measured. Sodium perchlorate and sodium iodide were selected as representative ion pairs for measuring the binding cooperativity of **MC1**. Both ion pairs consist of singly charged ions that are spherical (Na^+, I^-) or pseudo-spherical (ClO_4^-) and have reasonably good solubility in organic solvents. Unlike the previous studies employing turn-on factors, the quantification of cooperativity (Figure 7) demands[4,26] an accurate means of evaluating all the binding equilibria.

Titrations conducted for qualitative assessments of cooperativity (see Figures 3 and 4 and Supporting Information) were then analyzed quantitatively to obtain ΔG_{anion}, ΔG_{cation}, and $\Delta G_{overall}$, respectively. All of the titration data were fitted using HypNMR by following the changing chemical shift positions of multiple protons (Supporting Information). For the titrations with $TBAClO_4$, TBAI, $NaBPh_4$, $NaClO_4$, and NaI, multiple equilibria (ion binding, ion pairing, and ion-pair complexation) were included. For example, fitting the ClO_4^- anion titration includes the anion binding, K_{anion} (eq 10), the native ion pairing of $TBAClO_4$, K_{ip} (eq 11), and the ion-pair complexation of the receptor−anion complex with the countercation, K_{ipc} (eq 12). The ion-pairing constants, K_{ip}, of titrated salts ($TBAClO_4$, TBAI, $NaBPh_4$, $NaClO_4$, and NaI) were measured in separate experiments and used as fixed values in the fitting to simplify refinements and enhance accuracy (see Supporting Information for determination of K_{ip}).

$$\mathbf{MC} + X^- \rightleftharpoons \mathbf{MC}{\cdot}X^- \qquad K_{anion} \quad (10)$$

$$M^+ + X^- \rightleftharpoons MX \qquad K_{ip} \quad (11)$$

$$\mathbf{MC}{\cdot}X^- + M^+ \rightleftharpoons \mathbf{MC}{\cdot}MX \qquad K_{ipc} \quad (12)$$

The results of the titrations (Table 1) show that receptor **MC1** has moderate affinities for ClO_4^- (50 M^{-1}) and Na^+ (50 M^{-1}) but shows strong ion-pair binding (10^6 M^{-2}) indicating positive cooperativity. The cooperativity factor for **MC1** with $NaClO_4$, $\alpha(NaClO_4)$, was determined to be 400 ($= \beta_{overall}/K_{anion}K_{cation}$ = 1 000 000 M^{-2}/50 M^{-1} × 50 M^{-1})) with a corresponding free energy $\Delta G_\alpha(NaClO_4) = -15 \pm 1$ kJ mol^{-1}. For NaI, the I^- affinity was 50% higher at 80 M^{-1}, but the cooperativity factor was enhanced 3-fold to 1300 with $\Delta G_\alpha(NaI) = -18 \pm 1$ kJ mol^{-1}.

Since multiple equilibria were involved in determining the cooperativity, we conducted titrations with the anion-binding control macrocycle **MC2** (Figure 1) to test the validity of our model. This macrocycle is isosteric with **MC1** but it only bears a binding pocket for anions. Consistently, the anion affinities

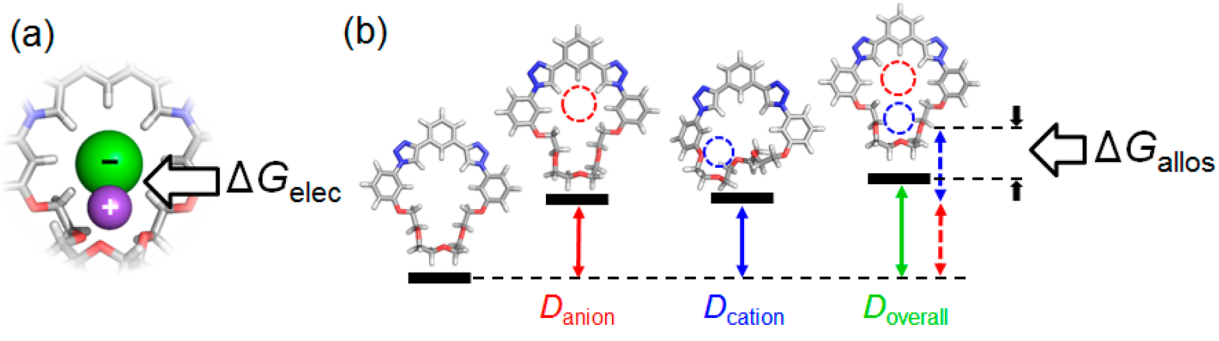

Figure 8. (a) Representation of electrostatic cooperativity, ΔG_{elec}, in ion-pair binding. (b) Representation of conformational allostery, ΔG_{allos}, as the difference between $D_{overall}$ and the sum of $D_{anion} + D_{cation}$, where D_i is the deformation energy penalty for each state i.

DOI: 10.1021/jacs.5b05839
J. Am. Chem. Soc. 2015, 137, 9746−9757

Table 1. Equilibrium Constants for Ion-Pair Binding of $NaClO_4$ and NaI to MC1 and MC2 (CD_2Cl_2:CD_3CN = 4:1, 298 K)[a]

	ion-pair receptor **MC1**	anion receptor **MC2**[b]
ClO_4^-, K_{anion} (M^{-1})	50 ± 10	60 ± 40
Na^+, K_{cation} (M^{-1})	50 ± 30	
$NaClO_4$, $\beta_{overall}$ (M^{-2})	1 000 000 ± 600 000	<10 000
cooperativity α	400 ± 250	
I^-, K_{anion} (M^{-1})	80 ± 5	100 ± 10
Na^+, K_{cation} (M^{-1})	50 ± 30	
NaI, $\beta_{overall}$ (M^{-2})	5 000 000 ± 1 000 000	<8000
cooperativity α	1300 ± 600	

[a]Ion pairing was also included in the fits to the model: K_{ip} ($TBAClO_4$ = 250 ± 60 M^{-1}, $NaBPh_4$ = 2 ± 1 M^{-1}, $NaClO_4$ = 200 ± 50 M^{-1}, TBAI = 80 ± 10 M^{-1}, and NaI = 60 ± 10 M^{-1}). [b]Fitting gives an upper limit for $\beta_{overall}$ (**MC2**).

are similar between **MC1** and **MC2**. Furthermore, **MC2** is not an ion-pair receptor, and measurements confirm **MC2** is significantly weaker than **MC1** at binding ion pairs (Table 1). The low $\beta_{overall}$ values for **MC2** are believed to be the product of weak anion binding ($K_{anion} \approx 50$) and weak pairing between the negatively charged complex **MC2**·X^- and Na^+ ion. This pairing likely produces an outer-sphere complex with the countercation:

$$\textbf{MC2}\cdot X^- + Na^+ \rightleftharpoons [\textbf{MC2}\cdot X^- \cdots Na^+], \quad K < 200\ M^{-1} \tag{13}$$

The similarities and differences between **MC1** and **MC2** verify that our method of analysis is able to resolve anion binding from ion-pair binding in order to assess them separately.

The smaller ionic size of I^- (r = 2.1 Å) relative to ClO_4^- (r = 2.4 Å), as determined from thermochemical radii,[42] is consistent with the greater cooperativity in binding NaI. Given the fact that all these ions are singly charged and the cooperativity was determined in the same solvent mixture, the principal difference between ion pairs is the charge separation distance. Assuming the positive and negative charges are located at the center of the ions and that solution structures resemble those in the solid state (Figure 9a), the shorter charge separation distance in the **MC1**·NaI complex matches its higher cooperativity (Figure 9b). It is remarkable that the ratio of ion–ion distances is close to the inverse ratio of cooperativity: $d_{NaClO_4}/d_{NaI} \approx \Delta G_{\alpha,NaI}/\Delta G_{\alpha,NaClO_4}$ (Figure 9b). That is, Coulomb's law correlates with the observed cooperativity difference even though it overestimates the absolute values by 9 kJ mol^{-1}: $E_{Coul}(NaI) = -27$ kJ mol^{-1} and $E_{Coul}(NaClO_4) = -24$ kJ mol^{-1}.

To summarize the experimental findings, **MC1** binds $NaClO_4$ and NaI with the same geometry but the cooperativity of NaI is stronger than $NaClO_4$. The distance dependence of the cooperativity hints at electrostatic attraction as the origin of the differences in cooperativity. However, Coulomb's law overestimates the cooperativity. There could be two possible explanations for this overestimation. Ion-pair binding to **MC1** may have 9 kJ mol^{-1} of *negative* allostery, making the net cooperativity smaller than Coulomb's law predictions. Alternatively, when the ions are bound inside **MC1**, their charges are diluted by multiple secondary interactions within the receptor (e.g., hydrogen-bonding and ion–dipole). As a result, the effective ionic charges are less than 1, which makes the attraction weaker than Coulomb's law. Experiments cannot differentiate between these two hypotheses. Testing requires deeper analysis with the aid of computational studies to calculate allostery and include all the secondary interactions. These computations allow us to test if the distance dependence originates from electrostatics and if Coulomb's law is a good predictor of electrostatic cooperativity.

Computational Analysis of Cooperativity in Ion-Pair Binding. A parallel approach to analyzing the cooperativity was undertaken by using calculations to help deconvolute

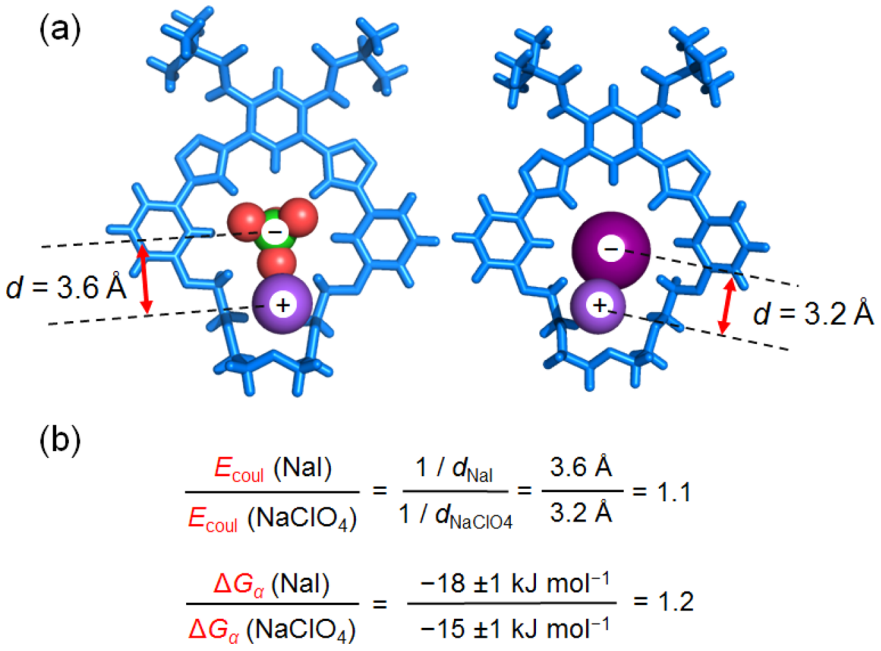

Figure 9. (a) Comparison of ion–ion separation distances in the crystal structures and (b) their impact on the expected Coulombic interactions, E_{Coul}, relative to observed cooperativities, ΔG_α.

DOI: 10.1021/jacs.5b05839
J. Am. Chem. Soc. 2015, 137, 9746–9757

conformational allostery from electrostatic cooperativity. The computational study was based on the same binding model as experiments (Figure 7 and eqs 3−7). Three simplifications were undertaken. First, we used model receptor **MC5** without side chains (Figure 1) as an isosteric version of **MC1**. Second, the ion pairs studied in the calculations involved spherical ions: NaCl, NaBr, and NaI. One unresolved issue emerged when studying nonspherical ions like ClO_4^-. They are believed to be rapidly tumbling[18c,e,f,43] within the receptor, and this averaging factor could not be readily accounted for in the present computational approach.[44] Third, a solvation model using CH_2Cl_2 was selected for being closest to the 4:1 CH_2Cl_2:CH_3CN mixture used experimentally. With these simplifications, the calculations will not provide absolute values for matching the experiment. Rather, the computational study is a self-consistent analysis that can provide insight on the origin of the ion−ion size dependence and on the accuracy of Coulomb's law predictions.

The binding energies, ΔE_{ion} (Figure 10a), associated with each guest were obtained from geometry-optimized structures

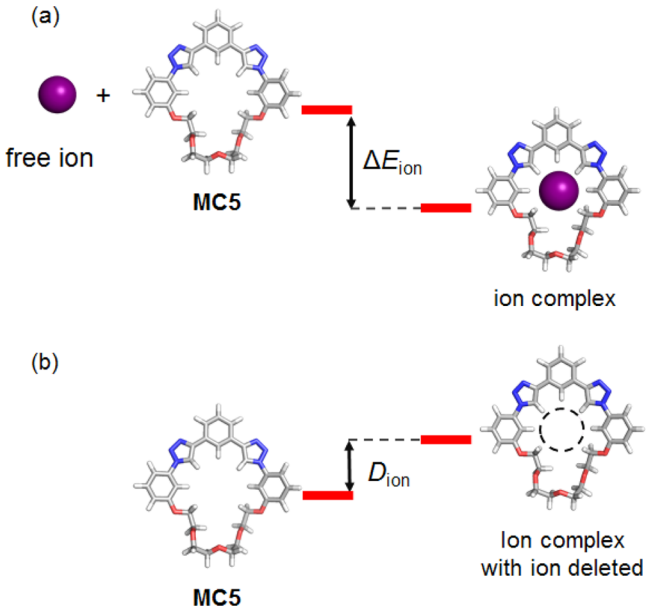

Figure 10. Energy diagrams illustrating how (a) binding energy, ΔE_{ion}, is obtained from the optimized geometries of reactants and products, and (b) deformation penalty, D_{ion}, is defined by the difference in energies for the receptors in the geometry of the empty macrocycle and when the macrocycle is complexed.

of the reactants (free **MC5** and free guest) and the product (**MC5**·guest complex). The deformation penalties, D_{ion}, associated with the binding events were determined in a similar way (Figure 10b). Deformation penalties were calculated as the difference in energy between the optimized geometry of free **MC5** and the geometry of the **MC5**·guest complex with the guest deleted from the structure.

In the computational study, every species (**MC5**, **MC5**·X^-, **MC5**·Na^+, and **MC5**·NaX) was optimized both in the gas phase and with CH_2Cl_2 solvation model to give structures, binding energies, and deformation penalties for the two phases. The geometries in the gas phase did not show significant changes upon solvation. The anion binding energies (Table 2) reduce to ∼30% upon CH_2Cl_2 solvation. Interestingly, the gas-phase binding of Na^+ (Table 2) is stronger than the anions but

Table 2. DFT Calculated Binding Energies, Δ*E*, and Deformation Penalties, *D*, in kJ mol^{-1} for MC5

		gas phase		CH_2Cl_2 solvation	
M^+	X^-	ΔE^{gas}	D^{gas}	ΔE^{sol}	D^{sol}
	Cl^-	−212	16	−58	9
	Br^-	−189	13	−51	6
	I^-	−172	11	−52	5
Na^+		−246	48	−39	29
Na^+	Cl^-	−767	24	−156	21
Na^+	Br^-	−737	22	−145	20
Na^+	I^-	−711	23	−140	19

reduces more significantly upon solvation to be weaker than the anions. The deformation penalties are generally less sensitive to solvation (Table 2). The following discussion will highlight the structures and values obtained with solvation model. The gas-phase structures can be found in the Supporting Information, and the gas-phase values are included in the main text. All the trends seen with solvation also hold true for the gas phase.

The geometries and the related energies (Table 2) of the ion complexes provide the basis from which to evaluate cooperativity. Optimized geometries of anion-bound complexes **MC5**·X^- (X^- = Cl^-, Br^-, and I^-) have similar structures (Figure 11). Anions sit inside the macrocycle held by triazole CH hydrogen-bonding, with CH···X^- distances ranging from 2.4 to 2.9 Å. The binding energies scale with anion size (Table 2). The **MC5**·Na^+ structure (Figure 11d) shows how the cation forms close contacts with four oxygen atoms in the glycol chain leaving one oxygen atom outside the cation-binding cavity.

The anion-binding site is more rigid while the cation-binding glycol is more flexible. Consistently, the deformation penalties, D_{ion} (Table 2), for binding anions are small and close to each other: D_X^{sol} ranges from 5 to 9 kJ mol^{-1}. The cation binding has a higher deformation penalty, D_{Na}^{sol} = 29 kJ mol^{-1}, which is attributed to glycol flexibility.

Geometries of complexes formed with the ion pairs (Figure 12) show anions and cations in direct contact. The binding energies of ion pairs follow similar trends as seen for anion binding. Their charge separation distances, $d_{complex}$ (Table 3), are very close to the values obtained with the ion pairs optimized in the absence of the receptor, $d_{free\ pair}$. The flexible glycol in **MC5** reorganizes to accommodate the bound pairs which have direct contact. The deformation penalties for ion-pair binding are in between those for the anions and cation.

The overall and allosteric cooperativity of ion-pair binding (Table 3) was determined (analogous to eq 6) using the data in Table 2. The electrostatic cooperativity, ΔE_{elec}, was then calculated using $\Delta E_{elec} = \Delta E_\alpha - \Delta E_{allos}$. Contrary to our first hypothesis, we find both allostery and electrostatic cooperativity are positive. While both these factors get smaller when the system is solvated, the electrostatic contribution is more sensitive to solvation. Nevertheless, the conformational allostery, ΔE_{allos}, of **MC5** binding NaCl, NaBr, and NaI remains smaller than electrostatics (ΔE_{allos} is 20−30% of ΔE_{elec}) in the CH_2Cl_2 solvent. It also shows a smaller (2 kJ mol^{-1}) variation across the ion pairs. Therefore, net cooperativity, ΔE_α, variation of 10 kJ mol^{-1} across the series NaCl, NaBr, and NaI mainly stems from variations in the electrostatic contribution (8 kJ mol^{-1}). Consequently, the electrostatic contribution to cooperativity dominates the decreasing trend in cooperativity.

DOI: 10.1021/jacs.5b05839
J. Am. Chem. Soc. 2015, 137, 9746−9757

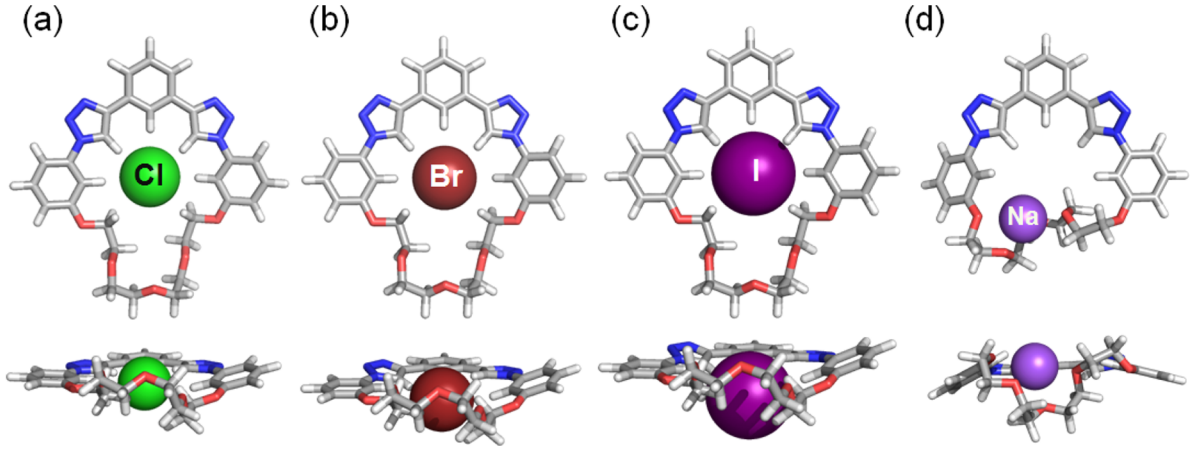

Figure 11. Geometry-optimized structures of (a) **MC5**·Cl^-, (b) **MC5**·Br^-, (c) **MC5**·I^-, and (d) **MC5**·Na^+.

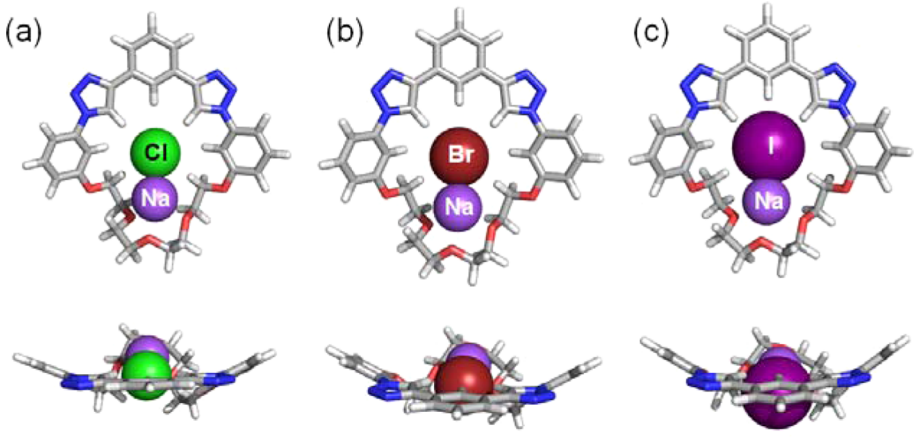

Figure 12. Geometry-optimized structures of **MC5** with (a) NaCl, (b) NaBr, and (c) NaI.

Table 3. Calculated Binding Cooperativity, ΔE_α, Conformational Allostery, ΔE_{allos}, and Electrostatic Cooperativity, ΔE_{elec}, All in kJ mol^{-1}, and Charge Separation Distances within MC5·Ion-Pair Complexes, $d_{complex}$, and Free Pairs, $d_{free\ pair}$, in Å, in Gas and Solvent Phases

	ΔE_α	ΔE_{allos}	ΔE_{elec}	$d_{complex}$	$d_{free\ pair}$	$\sum r_{ion}$ [a]
			Gas Phase			
NaCl	−309	−40	−269	2.5	2.4	2.7
NaBr	−302	−39	−263	2.7	2.5	2.8
NaI	−292	−36	−256	2.9	2.7	3.1
			CH_2Cl_2 Solvent			
NaCl	−59	−17	−42	2.7	2.6	2.7
NaBr	−55	−15	−40	2.8	2.8	2.8
NaI	−49	−15	−34	3.1	3.0	3.1

[a] $\sum r_{ion} = r_{Na} + r_X$ (X = Cl, Br, I), where r_{Cl} = 1.7 Å, r_{Br} = 1.8 Å, r_I = 2.1 Å, and r_{Na} = 1.0 Å.

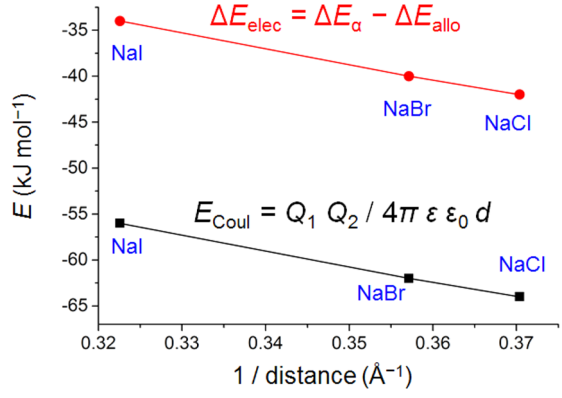

Figure 13. Plots of electrostatic cooperativity determined computationally, ΔE_{elec} (red), and from Coulomb's law, E_{Coul} (black), as a function of the charge separation distances, $1/d_{complex}$, derived from the optimized **MC5**·ion-pair complexes using CH_2Cl_2 as solvent medium.

Interpretation of Observed and Computed Cooperativity. The calculations (Table 3) show that electrostatic cooperativity is dominated by the charge separation distances, $d_{complex}$, as suggested by Coulomb's law (eq 1). This is a simple model that is based on a contacting ion pair with the macrocycle omitted. Coulomb's law would also have given the variation of electrostatic cooperativity with ion−ion distance (Figure 13, black line). However, the presence of other interactions present inside the binding cavity of the macrocycle (e.g., hydrogen-bonding and ion−dipole) would not be included. The computational model incorporates all these interactions and thus offers a more accurate estimate of electrostatic cooperativity, ΔE_{elec}, for the ion-pair binding within **MC5**. Ion−ion distance is seen to dictate the trend in ΔE_{elec} across the halide series (Figure 13, red line). However, the absolute value is less than from a Coulomb's law prediction by ∼20 kJ mol^{-1}. We attribute this difference to the secondary interactions present within the receptor−anion−cation ternary

DOI: 10.1021/jacs.5b05839
J. Am. Chem. Soc. 2015, 137, 9746−9757

complex that dilute the effective charges of the ions to be less than 1.

The electrostatic cooperativity, ΔE_{elec}, is dictated by anion−cation distance, $d_{complex}$, which can be correlated with the size of the constituent ions, $\sum r_{ion}$ (Table 3). This correlation arises as a consequence of the semiflexible character of macrocycle **MC5**. The macrocycle allows the ions to optimize their electrostatic interaction by contacting each other. Consistent with this idea, the internuclear distance in the complex, $d_{complex}$, is similar to the ion−ion distances of free ion pairs, $d_{free\ pair}$ (Table 3). Consequently, in semiflexible receptors where ion pairs have direct contact, electrostatic cooperativity is tuned by ionic sizes. This finding also explains the experimental observation that the smaller NaI ion pair has higher cooperativity than $NaClO_4$ within **MC1**.

Summarizing the computational study, it was found that complexes with NaCl, NaBr, and NaI have very similar geometries but their cooperativities decrease. This trend matches the experiments conducted with NaI and $NaClO_4$, and questions raised by experiment have been answered with calculations. First, the difference in cooperativity originates from electrostatics; allostery contributes to the cooperativity but it has minimal variation across the series (NaCl−NaI). The electrostatic cooperativity depends on ion−ion distance within the semiflexible receptor. Second, Coulomb's law can only predict the *trend* of electrostatic cooperativity; it overestimates the absolute value of cooperativity by missing secondary interactions. Finally it was revealed that allostery is less sensitive to solvation. As a consequence, increasing solvent polarity may reduce the electrostatic contribution significantly while having a smaller effect on allostery.

We further postulate that with a rigid receptor, which cannot reorganize itself, there may exist only a few ion pairs that will allow ion binding into the separate ion pockets at the same time as directing ion pairs to make contact. This situation is expected to give rise to peak selectivity for those few ion pairs. Many previously reported rigid ion pair receptors showing various selectivities appeared to take advantage of this design principle.[20a,23,25b,27,45] Our computational analysis also reveals that the electrostatic term, ΔE_{elec}, included in eq 8, contains contributions from pure ion−ion electrostatic attraction in addition to the secondary interactions. These secondary effects will always lessen electrostatic attraction and its ensuing impact on the cooperativity of binding contact ion pairs in receptors.

CONCLUSIONS

Cooperativity is the central concept in ion-pair binding, yet only a few studies have focused on quantitatively evaluating the degree and origin of cooperativity. In this work, we established a binding model that allowed experimental and computational analyses to be used together for a comprehensive examination of cooperativity in ion-pair binding. Our method is capable of generating more quantitative information on ion-pair binding than conventional turn-on factors. For the first time, the cooperativity factor was determined experimentally from thermodynamic quantifications of anion, cation, and overall ion-pair binding. It was found that NaI has higher cooperativity than $NaClO_4$ in our model system. Using density functional theory calculations, we provided the first separate examination of conformational allostery and electrostatic cooperativity. This study revealed that the size of the ions dictated the electrostatic cooperativity but only if the ions could make direct contact with each other. Coulomb's law could predict the trend of electrostatic cooperativity but overestimated the absolute value by not accounting for the putative charge dilution that occurs when the ions bind to their respective anion/cation sites. The analyses and findings presented here provide a new approach for the investigation of cooperativity that is expected to aid in the future rational designs and understanding of receptor-mediated ion-pair binding.

ASSOCIATED CONTENT

Supporting Information

Computational methods, syntheses, NMR data, titration analyses, X-ray data, and optimized structures. The Supporting Information is available free of charge on the ACS Publications website at DOI: 10.1021/jacs.5b05839.

AUTHOR INFORMATION

Corresponding Author

*aflood@indiana.edu

Notes

The authors declare no competing financial interest.

ACKNOWLEDGMENTS

The authors gratefully acknowledge support by the Chemical Science, Geosciences and Biosciences Division, Office of Basic Energy Sciences, U.S. Department of Energy (DE-FG02-09ER16068). Y.L. thanks the Raymond Siedle Materials Fellowship for support. J.R.A. thanks Indiana University for summer research scholarship for support.

REFERENCES

(1) Lehn, J.-M. *Supramolecular Chemistry: Concepts and Perspectives*; VCH: Weinheim, 1995.

(2) Smith, B. D. Ion Pair Recognition by Ditopic Receptors. In *Macrocyclic Chemistry: Current Trends and Future Prospectives*; Gloe, K., Antonioli, B., Eds.;; Kluwer: London, 2005.

(3) Kovbasyuk, L.; Krämer, R. *Chem. Rev.* **2004**, *104*, 3161−3188.

(4) (a) Wintergerst, M. P.; Levitskaia, T. G.; Moyer, B. A.; Sessler, J. L.; Delmau, L. H. *J. Am. Chem. Soc.* **2008**, *130*, 4129−4139. (b) Aydogan, A.; Coady, D. J.; Kim, S. K.; Akar, A.; Bielawski, C. W.; Marquez, M.; Sessler, J. L. *Angew. Chem., Int. Ed.* **2008**, *47*, 9648−9652. (c) McConnell, A. J.; Beer, P. D. *Angew. Chem., Int. Ed.* **2012**, *51*, 5052−5061. (d) Romanski, J.; Piatek, P. *Chem. Commun.* **2012**, *48*, 11346−11348. (e) McDonald, K. P.; Qiao, B.; Twum, E. B.; Lee, S.; Gamache, P. J.; Chen, C.-H.; Yi, Y.; Flood, A. H. *Chem. Commun.* **2014**, *50*, 13285−13288.

(5) (a) Tong, C. C.; Quesada, R.; Sessler, J. L.; Gale, P. A. *Chem. Commun.* **2008**, 6321−6323. (b) Davis, J. T.; Okunola, O.; Quesada, R. *Chem. Soc. Rev.* **2010**, *39*, 3843−3862. (c) Kim, D. S.; Sessler, J. L. *Chem. Soc. Rev.* **2015**, *44*, 532−546.

(6) (a) Rauniyar, V.; Lackner, A. D.; Hamilton, G. L.; Toste, F. D. *Science* **2011**, *334*, 1681−1684. (b) Mahlau, M.; List, B. *Angew. Chem., Int. Ed.* **2013**, *52*, 518−533. (c) Brak, K.; Jacobsen, E. N. *Angew. Chem., Int. Ed.* **2013**, *52*, 534−561.

(7) Gokel, G. W. Molecular Recognition Receptors for Cationic Guests. In *Comprehensive Supramolecular Chemistry*; Lehn, J.-M., Atwood, J. L., Davies, J. E. D., MacNicol, D. D., Vogtle, F., Eds.; Pergamon: Oxford, 1996; Vol. *1*.

(8) (a) Sessler, J. L.; Gale, P. A.; Cho, W.-S. *Anion Receptor Chemistry*; Royal Society of Chemistry: Cambridge, 2006. (b) Gale, P. A.; Busschaert, N.; Haynes, C. J. E.; Karagiannidis, L. E.; Kirby, I. L. *Chem. Soc. Rev.* **2014**, *43*, 205−241.

(9) (a) Li, Y.; Flood, A. H. *Angew. Chem., Int. Ed.* **2008**, *47*, 2649−2652. (b) Li, Y.; Flood, A. H. *J. Am. Chem. Soc.* **2008**, *130*, 12111−12122.

DOI: 10.1021/jacs.5b05839
J. Am. Chem. Soc. 2015, 137, 9746−9757

(10) Sessler, J. L.; Gross, D. E.; Cho, W.-S.; Lynch, V. M.; Schmidtchen, F. P.; Bates, G. W.; Light, M. E.; Gale, P. A. *J. Am. Chem. Soc.* **2006**, *128*, 12281−12288.
(11) (a) Bianchi, A.; Bowman-James, L.; García-España, E. *Supramolecular Chemistry of Anions*; Wiley-VCH: New York, 1997. (b) Beer, P. D.; Gale, P. A.; Smith, D. K. *Supramolecular Chemistry*; Oxford: New York, 1999. (c) Hua, Y.; Ramabhadran, R. O.; Uduehi, E. O.; Karty, J. A.; Raghavachari, K.; Flood, A. H. *Chem. - Eur. J.* **2011**, *17*, 312−321. (d) Hua, Y.; Liu, Y.; Chen, C.-H.; Flood, A. H. *J. Am. Chem. Soc.* **2013**, *135*, 14401−14412.
(12) Comarmond, J.; Plumere, P.; Lehn, J.-M.; Agnus, Y.; Louis, R.; Weiss, R.; Kahn, O.; Morgenstern-Badarau, I. *J. Am. Chem. Soc.* **1982**, *104*, 6330−6340.
(13) Kim, S. K.; Sessler, J. L. *Chem. Soc. Rev.* **2010**, *39*, 3784−3809.
(14) Douglass, E. F.; Miller, C. J.; Sparer, G.; Shapiro, H.; Spiegel, D. A. *J. Am. Chem. Soc.* **2013**, *135*, 6092−6099.
(15) (a) Yoon, D.-W.; Gross, D. E.; Lynch, V. M.; Sessler, J. L.; Hay, B. P.; Lee, C.-H. *Angew. Chem., Int. Ed.* **2008**, *47*, 5038−5042. (b) Kim, S. K.; Sessler, J. L.; Gross, D. E.; Lee, C.-H.; Kim, J. S.; Lynch, V. M.; Delmau, L. H.; Hay, B. P. *J. Am. Chem. Soc.* **2010**, *132*, 5827−5836. (c) Cai, J.; Hay, B. P.; Young, N. J.; Yang, X.; Sessler, J. L. *Chem. Sci.* **2013**, *4*, 1560−1567. (d) Kim, S. K.; Lynch, V. M.; Hay, B. P.; Kim, J. S.; Sessler, J. L. *Chem. Sci.* **2015**, *6*, 1404−1413.
(16) (a) Sachleben, R. A.; Bryan, J. C.; Engle, N. L.; Haverlock, T. J.; Hay, B. P.; Urvoas, A.; Moyer, B. A. *Eur. J. Org. Chem.* **2003**, *2003*, 4862−4869. (b) Hay, B. P.; Gutowski, M.; Dixon, D. A.; Garza, J.; Vargas, R.; Moyer, B. A. *J. Am. Chem. Soc.* **2004**, *126*, 7925−7934. (c) Hay, B. P.; Firman, T. K.; Moyer, B. A. *J. Am. Chem. Soc.* **2005**, *127*, 1810−1819.
(17) (a) Custelcean, R.; Bosano, J.; Bonnesen, P. V.; Kertesz, V.; Hay, B. P. *Angew. Chem., Int. Ed.* **2009**, *48*, 4025−4029. (b) Custelcean, R.; Bonnesen, P. V.; Duncan, N. C.; Zhang, X.; Watson, L. A.; Van Berkel, G.; Parson, W. B.; Hay, B. P. *J. Am. Chem. Soc.* **2012**, *134*, 8525−8534. (c) Jia, C.; Hay, B. P.; Custelcean, R. *Inorg. Chem.* **2014**, *53*, 3893−3898.
(18) (a) Bandyopadhyay, I.; Raghavachari, K.; Flood, A. H. *ChemPhysChem* **2009**, *10*, 2535−2540. (b) Hua, Y.; Ramabhadran, R. O.; Karty, J. A.; Raghavachari, K.; Flood, A. H. *Chem. Commun.* **2011**, *47*, 5979−5981. (c) Ramabhadran, R. O.; Hua, Y.; Flood, A. H.; Raghavachari, K. *Chem. - Eur. J.* **2011**, *17*, 9123−9129. (d) McDonald, K. P.; Ramabhadran, R. O.; Lee, S.; Raghavachari, K.; Flood, A. H. *Org. Lett.* **2011**, *13*, 6260−6263. (e) Ramabhadran, R. O.; Hua, Y.; Flood, A. H.; Raghavachari, K. *J. Phys. Chem. A* **2014**, *118*, 7418−7423. (f) Ramabhadran, R. O.; Liu, Y.; Hua, Y.; Ciardi, M.; Flood, A. H.; Raghavachari, K. *J. Am. Chem. Soc.* **2014**, *136*, 5078−5089.
(19) (a) Scheerder, J.; van Duynhoven, J. P. M.; Engbersen, J. F. J.; Reinhoudt, D. N. *Angew. Chem., Int. Ed. Engl.* **1996**, *35*, 1090−1093. (b) Gavette, J. V.; Lara, J.; Reling, L. L.; Haley, M. M.; Johnson, D. W. *Chem. Sci.* **2013**, *4*, 585−590. (c) Howe, E. N. W.; Bhadbhade, M.; Thordarson, P. *J. Am. Chem. Soc.* **2014**, *136*, 7505−7516. (d) Kim, S. K.; Sessler, J. L. *Acc. Chem. Res.* **2014**, *47*, 2525−2536. (e) Saha, I.; Park, K. H.; Han, M.; Kim, S. K.; Lynch, V. M.; Sessler, J. L.; Lee, C.-H. *Org. Lett.* **2014**, *16*, 5414−5417.
(20) (a) Mahoney, J. M.; Beatty, A. M.; Smith, B. D. *J. Am. Chem. Soc.* **2001**, *123*, 5847−5848. (b) Kim, S. K.; Lynch, V. M.; Young, N. J.; Hay, B. P.; Lee, C.-H.; Kim, J. S.; Moyer, B. A.; Sessler, J. L. *J. Am. Chem. Soc.* **2012**, *134*, 20837−20843.
(21) Coulomb, C. A. *Histoire de l'Académie Royale des Sciences*; Imprimerie Royale: Paris, 1788; pp 569−577.
(22) (a) Ni, X.-L.; Rahman, S.; Zeng, X.; Hughes, D. L.; Redshaw, C.; Yamato, T. *Org. Biomol. Chem.* **2011**, *9*, 6535−6541. (b) Valderrey, V.; Escudero-Adán, E. C.; Ballester, P. *Angew. Chem., Int. Ed.* **2013**, *52*, 6898−6902.
(23) Deetz, M. J.; Shang, M.; Smith, B. D. *J. Am. Chem. Soc.* **2000**, *122*, 6201−6207.
(24) Beer, P. D.; Drew, M. G. B.; Knubley, R. J.; Ogden, M. I. *J. Chem. Soc., Dalton Trans.* **1995**, 3117−3123.
(25) (a) Lankshear, M. D.; Cowley, A. R.; Beer, P. D. *Chem. Commun.* **2006**, 612−614. (b) Romanski, J.; Piatek, P. *J. Org. Chem.* **2013**, *78*, 4341−4347.
(26) Roelens, S.; Vacca, A.; Francesconi, O.; Venturi, C. *Chem. - Eur. J.* **2009**, *15*, 8296−8302.
(27) Perraud, O.; Robert, V.; Martinez, A.; Dutasta, J.-P. *Chem. - Eur. J.* **2011**, *17*, 4177−4182.
(28) (a) Shi, D.; Schwall, C.; Sfintes, G.; Thyrhaug, E.; Hammershøj, P.; Cárdenas, M.; Simonsen, J. B.; Laursen, B. W. *Chem. - Eur. J.* **2014**, *20*, 6853−6856. (b) Haketa, Y.; Sasaki, S.; Ohta, N.; Masunaga, H.; Ogawa, H.; Mizuno, N.; Araoka, F.; Takezoe, H.; Maeda, H. *Angew. Chem., Int. Ed.* **2010**, *49*, 10079−10083. (c) González-Rodríguez, D.; van Dongen, J. L. J.; Lutz, M.; Spek, A. L.; Schenning, A. P. H. J.; Meijer, E. W. *Nat. Chem.* **2009**, *1*, 151−155.
(29) Frisch, M. J.; et al. *Gaussian Development Version*, Revision H.32; Gaussian Inc.: Wallingford, CT, 2010.
(30) Zhao, Y.; Truhlar, D. G. *Theor. Chem. Acc.* **2008**, *120*, 215−241.
(31) Mennucci, B.; Tomasi, J. *J. Chem. Phys.* **1997**, *106*, 5151−5158.
(32) Check, C. E.; Faust, T. O.; Bailey, J. M.; Wright, B. J.; Gilbert, T. M.; Sunderlin, L. S. *J. Phys. Chem. A* **2001**, *105*, 8111−8116.
(33) Lee, S.; Hua, Y.; Park, H.; Flood, A. H. *Org. Lett.* **2010**, *12*, 2100−2102.
(34) (a) Rostovtsev, V. V.; Green, L. G.; Fokin, V. V.; Sharpless, K. B. *Angew. Chem., Int. Ed.* **2002**, *41*, 2596−2599. (b) Tornøe, C. W.; Christensen, C.; Meldal, M. *J. Org. Chem.* **2002**, *67*, 3057−3064.
(35) Andersen, J.; Madsen, U.; Björkling, F.; Liang, X. *Synlett* **2005**, 2209−2213.
(36) (a) Amini, M. K.; Shamsipur, M. *J. Phys. Chem.* **1991**, *95*, 9601−9604. (b) Izatt, R. M.; Pawlak, K.; Bradshaw, J. S.; Bruening, R. L. *Chem. Rev.* **1995**, *95*, 2529−2586. (c) Shamsipur, M.; Irandoust, M. *J. Solution Chem.* **2008**, *37*, 657−664.
(37) (a) Plenio, H.; Diodone, R. *J. Am. Chem. Soc.* **1996**, *118*, 356−367. (b) Khan, F. A.; Parasuraman, K.; Sadhu, K. K. *Chem. Commun.* **2009**, *45*, 2399−2401.
(38) Pedzisa, L.; Hay, B. P. *J. Org. Chem.* **2009**, *74*, 2554−2560.
(39) The chemical shift change of H_e at 4.4 ppm upon binding is greater than those of the other glycol protons in **MC1** (H_f, H_j, H_k), which display shifts attributed to the binding of Na^+.
(40) (a) Pascu, S. I.; Naumann, C.; Kaiser, G.; Bond, A. D.; Sanders, J. K. M.; Jarrosson, T. *Dalton Trans.* **2007**, 3874−3884. (b) Thatcher, R. J.; Johnson, D. G.; Slattery, J. M.; Douthwaite, R. E. *Chem. - Eur. J.* **2012**, *18*, 4329−4336. (c) Kang, H.; Facchetti, A.; Stern, C. L.; Rheingold, A. L.; Kassel, W. S.; Marks, T. J. *Org. Lett.* **2005**, *7*, 3721−3724.
(41) Maryott, A. A.; Smith, E. R. *Table of Dielectric Constants of Pure Liquids*; NBS Circular 514; National Bureau of Standards: Washington, DC, 1951.
(42) Roobottom, H. K.; Jenkins, H. D. B.; Passmore, J.; Glasser, L. *J. Chem. Educ.* **1999**, *76*, 1570.
(43) Hirsch, B. E.; Lee, S.; Qiao, B.; Chen, C.-H.; McDonald, K. P.; Tait, S. L.; Flood, A. H. *Chem. Commun.* **2014**, *50*, 9827−9830.
(44) As a consequence, we believe that the size of ClO_4^- present in the calculations is an underestimate of the averaged size of the tumbling anion characterized experimentally (Supporting Information).
(45) (a) Beer, P. D; Dent, S. W. *Chem. Commun.* **1998**, *34*, 825−826. (b) Park, I.-W.; Yoo, J.; Adhikari, S.; Park, J. S.; Sessler, J. L.; Lee, C.-H. *Chem. - Eur. J.* **2012**, *18*, 15073−15078. (c) Otón, F.; González, M. d. C.; Espinosa, A.; Ramírez de Arellano, C.; Tárraga, A.; Molina, P. *J. Org. Chem.* **2012**, *77*, 10083−10092.

DOI: 10.1021/jacs.5b05839
J. Am. Chem. Soc. 2015, 137, 9746−9757